Article

Not peer-reviewed version

Organic Matter Accelerated Microbial Iron Reduction and Available Phosphorus Release in Reflooded Paddy Soils

Xipeng Liu , Yuchen Shu , Kejie Li , Haotian Wang , Qingfang Bi , Haibo Wang , Chengliang Sun , Xianyong Lin *

Posted Date: 11 December 2023

doi: 10.20944/preprints202312.0664.v1

Keywords: manure application; P availability; soil biogeochemistry; microbial carbon mineralization; ironcarbon cycles

Article

Organic Matter Accelerated Microbial Iron Reduction and Available Phosphorus Release in Reflooded Paddy Soils

Xipeng Liu [1,2,#], Yuchen Shu [1,#], Kejie Li [1,#], Haotian Wang [3], Qingfang Bi [1,4], Haibo Wang [1], Chengliang Sun [1] and Xianyong Lin [1,*]

[1] MOE Key Laboratory of Environment Remediation and Ecological Health, College of Environmental and Resource Sciences, Zhejiang University, Hangzhou 310058, China
[2] Microbial Ecology cluster, Genomics Research in Ecology and Evolution in Nature (GREEN), Groningen Institute for Evolutionary Life Sciences (GELIFES), University of Groningen, 9747 AG Groningen, The Netherlands
[3] Thünen Institute of Biodiversity, D-38116, Braunschweig, Germany
[4] Max Planck Institute for Biogeochemistry, Jena, 07745, Germany
* Correspondence: authors: Xianyong Lin (xylin@zju.edu.cn)
[#] The authors contributed to the manuscript equally.

Abstract: The cycling of soil phosphorus (P) is inherently linked with soil organic carbon-iron (C-Fe) cycling, yet empirical integration of these processes within paddy soils remains scarce. In this study, we conducted a microcosm experiment using paddy soils subjected to six distinct fertilization regimes involving varying P inputs for five years. In addition to evaluating P activation under reflooding conditions, we assessed the Fe reduction process and characterized the properties of dissolved organic matter (DOM) at the molecular level using Fourier transform ion cyclotron resonance mass spectrometry (FT-ICR MS), alongside profiling the composition of soil microbial communities with high-throughput sequencing. Our findings revealed that after 25 days of reflooding, soil Olsen-P content increased by an average of 73% compared to its initial state, showing a strong correlation with the Fe reduction process. Specifically, treatments involving pig manure application exhibited higher Fe reduction rates and enhanced P activation, highlighting the role of organic matter in facilitating Fe reduction. Investigations on the relative abundance of typical iron-reducing microbes further supported their importance in P activation, but the rate of iron reduction is limited by soil organic matter content. Delving deeper into DOM properties, soil DOM composition profiling and network analysis suggested that high-molecular-weight DOM, particularly lignins, served as the primary resources driving Fe reduction by iron-reducing microbes, consequently promoting Fe reduction and P release. Taken together, our study assembled the C-Fe-P cycling dynamics in paddy soils, emphasizing the pivotal role of microbial-driven Fe reduction facilitated by soil DOM in P availability and subsequently sustainable agricultural practices.

Keywords: manure application; P availability; soil biogeochemistry; microbial carbon mineralization; iron–carbon cycles

1. Introduction

Phosphorus (P) is an essential nutrient that plays a crucial role in influencing crop growth and yield. In solution, P often exhibits a high adsorption capacity to iron (Fe) (hydr)oxides, which contributes to the extensive exploration and utilization of iron oxides for removing phosphorus from wastewater (Wilfert et al. 2015; Wang et al. 2023b). However, such a trait partly results in low P availability in both natural terrestrial and agricultural ecosystems (Borch and Fendorf 2007), restricting species survival and crop yields. Since P fertilizer resources (i.e., phosphate rock) are finite and dwindling and may be depleted within decades (Cordell et al. 2009), research on improving soil P availability in agricultural production has become more important and extensive than ever (Damon et al. 2014; Zhu et al. 2018).

 doi:10.20944/preprints202312.0664.v1

The application of organic fertilizer is a common method for improving soil P availability (Jindo et al. 2023), in addition to the direct input of organic phosphorus. The increasing of soil organic matter content can improve soil structure and water-holding capacity, promote the availability of phosphorus, and consequently, facilitate phosphorus absorption by plants. This findings has been validated in numerous field and greenhouse experiments (Yin and Liang 2013; Yan et al. 2016; Yang et al. 2017; Abboud et al. 2018). In terms of underlying mechanisms, dissolved organic matter (DOM) has been considered the one of primary factors influencing P availability and mobility, and it can be practically manipulated (Liu et al., 2019; Li et al., 2022; Jindo et al., 2023). Firstly, DOM has the capacity to solubilize or desorb P that tightly binds to soil particles by competing for binding sites on soil surfaces with P, thereby increasing the solubility of phosphorus and make it more accessible for plant absorption (Takahashi and Katoh 2022). Secondly, DOM can alter soil pH by interacting with hydrogen ions, potentially increasing the pH of acidic soils after utilization of DOM, which in turn can increase the solubility of P compounds (Penn and Camberato 2019). Thirdly, DOM serve as a carbon source that shapes soil microbes capable of releasing organic acids and enzymes, thereby enhancing the solubilization and mineralization of organic and inorganic forms of P (Zheng et al. 2019; Bi et al. 2020).

The properties of DOM, including molecular composition and weight, functional group, charge characteristics, and stability, exert a strong influence on the previously mentioned mechanisms that regulate phosphorus availability in soils. For instance, although both low- and high- molecular-weight (MW) components may theoretically increase P desorption from minerals through similar physicochemical processes such as pH modification, the forming of organic ligands, and competing for sorption sites (Hiemstra et al. 2013; Menezes-Blackburn et al. 2016; Ge et al. 2020). Recent studies suggest that high-molecular-weight component plays a more prominent role in P release. Specifically, many studies have revealed a significant and positive correlation between DOM humification degree and the maximum P adsorption capacity of in different soils (Liu et al. 2018; Long et al. 2021; Zhang et al. 2022; Li et al. 2022). A recent microcosm experiment provided direct evidence that the application of high-molecular-weight DOM (ultrafiltrated with a 1 kDa membrane) to soils reduced in a more substantial reduction in soil phosphorus sorption compared to low-molecular-weight DOM (Wang et al., 2023). However, these studies mainly focused on the physicochemical mechanism, whereas the biological mechanism of the interaction between DOM and microorganisms has been largely ignored. Therefore, it is crucial to investigate the relationship between DOM properties and P availability in a living soil containing active microorganisms to better understand the role of DOM in phosphorus activation, which is indispensable for sustainable management of both soil P and DOM.

Paddy soil exhibits a unique biogeochemical property characterized by cyclic wetting and drying which is different from other farmland soils. During the fluctuations between aerobic and anaerobic conditions, there can be significant shifts in soil pH, microbial activity, as well as the fate of DOM and metal oxides (Koegel-Knabner et al. 2010). These changes can have a profound impact on P availability. In this study, we aim to (1) bridge the soil P activation and microbe-driven Fe reduction and (2) investigate the effect of DOM properties in interacting with soil microbes on P availability and Fe reduction during the window of reflooding paddy soil. To address this issue, we conducted a microcosm experiment using reflooded paddy soil subjected to different fertilization regimes and assessed P activation. We adapted the Fourier transform ion cyclotron resonance mass spectrometry (FT-ICR MS) to characterize DOM properties at the molecular level and the high-throughput sequencing to profile the composition of soil microbial communities. We hypothesized that flooded paddy soils treated with organic manure exhibit a higher maximum Fe-reduction rate and can facilitate the available P release and high molecular weight DOM is shown to facilitate P releases through the acceleration of the Fe reduction process.

 doi:10.20944/preprints202312.0664.v1

2. Materials and methods

2.1. Field experimental design and soil sample collection

A long-term field experiment of a double-rice (*Oryza sativa* L.) rotation was started in 2013 and was located in Sixi Town, Jiangxi Province, China (115°07'13" E, 28°15'2" N). The experimental site and soil properties were described well in the previous publication (Li et al. 2022). Six fertilization regimes were included in this study: (1) CK, no fertilization; (2) NK, only fertilized with chemical N and K; (3) NPK, chemical NPK fertilization (conventional P dosage for this region); (4) M(20%P), only fertilized with manure, while the rate was equal to 20% P input of NPK treatment; (5) CM(P), replacing 20% chemical P with manure at the same total nutrient input as NPK treatment; (6) CM(-P), optimized fertilization by reducing the 20% chemical P application in comparison with CM(P) treatment. The total nutrient input through organic and inorganic fertilizers is presented in Table S1. The experiment was a completely randomized block with four replicates. The soil samples (0-20 cm) consisting of ten individual cores were collected from each block after crop harvest in November 2017. The composite samples were air-dried then ground to pass a 2-mm sieve for subsequent laboratory analyses. Soil physiochemical properties were assessed and reported previously (Li et al. 2022) and were shown in the Table S2.

2.2. Iron-reducing capacity under flooded conditions in microcosms

The iron-reducing capacity was assessed for soils with different fertilization treatments. All soil with a moisture of 60% of field capacity were pre-incubated at 25 °C in darkness for seven days. Thirty grams of soil were filled into the brown serum vial and followed by adding 30 ml of sterilized deionized water, capping with rubber septa and flushing with N2 for 10 min. Then, the aluminum-lid sealed vails were incubated at 25°C in darkness. The soil-water mixtures were sampled from vials at 0, 1, 2, 3, 5, 7, 10, 15, 20, and 25 days for concentration assessments of Fe(II) and soil available phosphorus (Olsen-P). For Fe(II) content, 0.4 mL of the sample suspension was mixed with 4.6 mL of 0.5 mol L-1 HCl solution and react in N2 for 24 h, and the Fe(II) concentration was measured by the O-phenanthroline spectrophotometry. For Olsen-P content, 0.4 mL of the sample suspension was mixed with 4.6 mL of 0.5 mol L-1 NaHCO3 solution and shake for 30 min, and the Olsen-P concentration was measured by the molybdenum blue method. The changed amount of Olsen-P (ΔOlsen-P) after 25 days compared to Day 0 was used as the P activation potential, and the ratio (ΔOlsen-P/TP) of Olsen-P content change after 25-day flooding to total P content (TP) at Day 0 was used to represent the P activation efficiency during iron reduction.

Iron reduction was fitted using the logistic equation, as it captures the microbial growth dynamics inherent in this biological process mediated by microorganisms (He and Qu 2008). The equation can be expressed as follows:

$$y = \frac{a}{1 + be^{-cx}}$$

where x is the incubation time (day), y is the content of Fe(II) (mg g-1), a is the maximum accumulation of Fe(II), indicating the maximum iron reduction potential (Pmax), b is the model parameter, c is the reaction velocity constant of Fe(II). The maximum reduction rate of iron (Vmax) was calculated as 0.25ac, and the time to reach the maximum iron reduction rate (Tmax) was calculated as Inb/c.

2.3. Extraction and molecular characterization of soil DOM

Soil sample collected from CK, NPK, and CM(-P) treatments, was mixed with ultrapure water at a ratio of 1:10 (w/v), and the mixture was shake at 25°C for 24 h and centrifuged at 4000 rpm for 20 min. The subsequent supernatant was filtered with a 0.45 μm microporous membrane to assess its DOC and DOM contents. DOC content was determined with a TOC instrument (TOC-L, Shimadzu, Japan). The rest of the DOM solution was immediately stored at 4°C for molecular characterization.

 doi:10.20944/preprints202312.0664.v1

The molecular characterization of DOM was performed using Fourier transform ion cyclotron resonance mass spectrometry (FT-ICR MS) combined with an in-house standard method to obtain reproducible results (He et al. 2020). Briefly, DOM samples were initially purified a solid-phase extraction process. The extraction column (Bond Elut-PPL, 500 mg, 6 mL, Agilent Technologies, United States) was prepared by activation with MS-grade methanol and HPLC-grade water (pH = 2). Subsequently, the DOM sample (pH = 2) was passed through a 0.45-μm extraction column, followed by wash with 3 column volumes of HPLC-grade water (pH = 2), dried with the blowing ultrapure N2, and a final elution with 1.5 column volumes of MS-grade methanol. Second, the MS analysis of DOM sample was carried out using a 9.4 T Bruker Apex-Ultra FT-ICR MS equipped with an electrospray ionization source, following the procedures indicated in He et al., 2020. The mass range was set at m/z 200–800 and the data size were set to 2 M words. To enhance the signal-to-noise ratio (S/N) of the mass spectrum, a total of 128 continuous scans were co-added for each analysis. Other parameters included a flight time of 1.3 ms, ionization voltage at 3500/3000 V, atomization gas flow rate of 2.0 L min-1, drying gas flow rate of 2.0 L min-1, and a drying gas temperature of 200°C.

2.4. Soil DNA extraction, 16S rRNA gene amplification, and high-throughput sequencing

Soil DNA from all treatments was extracted on the fourth day of the microcosm under flooding conditions. In brief, a total of 0.5 g soil was employed for the extraction of total DNA using the FastDNA® Spin Kit for Soil kit (MP Biomedical, USA). The base-tagged 515F (5'-GTGCCAGCMGCCGCGG-3') and 907R (5'-CCGTCAATTCMTTTRAGT-3') were used as forward and reverse primers for the PCR amplification of 16S rRNA gene (V4-V5 region) (Zhou et al. 2011). Agarose gel electrophoresis (2.0% w/v in TBE buffer) was utilized to verify the size and integrity of the PCR products, following the methodology outlined by Sambrook et al. (Sambrook and Russell 2006). The amplicons were purified using the Universal DNA Purification Kit, Tiangen, China), and were subsequently combined in equal concentration and sequenced on an Illumina Hiseq 2500 platform at Novogene in China.

The raw data of 16S rRNA sequences were filtered and analyzed using the QIIME pipeline (Kuczynski et al. 2011). The obtained reads were subjected to OTU (operational taxonomic unit) clustering analysis using mothur software (Schloss et al. 2009), with a similarity threshold at 97%. Representative sequences were then classified using the Silva database (Quast et al. 2013), with a confidence threshold of 0.8. Each sample was rarefied to a depth of 37,174 sequences. All the raw sequencing data have been deposited in the National Center for Biotechnology Information Sequence Read Archive under the accession number PRJNA756874.

2.5. Statistical analyses

We employed R (version 4.2.2) for data analyses and visualization. All statistically significant differences, such as for soil properties, bacterial biomass, abundance, and diversity, were determined with One-way analysis of variance (ANOVA) with Tukey's Post-Hoc test with R package "stats" and displayed with "multcompView" package (Graves and Dorai-Raj 2019). Variance Partitioning Analysis (VPA) was used to assess the driver of soil P activation efficiency and supply potential after reflooding with R package "vegan" (Oksanen et al. 2022).

The properties of DOM were calculated based on its stoichiometric and elemental constraints for each compound category. The double-bond equivalent (DBE/C), calculated by (2C–H+N+P+2)/2/C, indicates the density of C = C double bonds in a formula (Koch and Dittmar 2006; Tfaily et al. 2013). The modified aromaticity index (AI) is calculated by (1+C–0.5O–S–0.5H)/(C-0.5O-S-N-P) (Koch and Dittmar 2006; Chen et al. 2022). The boundary limits in the van Krevelen diagram were adapted for categorizing the assigned features based on AI, O/C, and H/C indexes (Li et al. 2018; Rivas-Ubach et al. 2018; Qiu et al. 2019), including (1) lipid-like compounds (O/C: 0–0.3, H/C: 1.5–2.0), (2) protein/amino sugar-like compounds (O/C: 0.3–0.67, H/C: 1.5–2.2), (3) carbohydrate-like compounds (O/C: 0.67–1.2, H/C:1.5–2.4), (4) lignin-like compounds (O/C: 0.1–0.67, H/C: 0.7–1.5), (5) tannin-like compounds (O/C: 0.67–1.2, H/C: 0.7–1.5), (6) condensed aromatic-like compounds (O/C: 0–0.67, H/C: 0.2–0.7), and (7) others (the compounds that do not belong to the above 6 groups).

 doi:10.20944/preprints202312.0664.v1

The potential iron-reducing microbes were classified according to previous studies (Weber et al. 2006; Chen et al. 2021; Yao et al. 2023) and were summarized in the Table S5. Network analysis was performed to reveal the potential association between DOM and iron-reducing microbes based on the correlation analysis by combining three treatments (CK, NPK, and CM(-P), n = 12). In brief, iron-reducing OTUs (average relative abundance > 0.01%) and DOM (average relative abundance > 0.01%) were selected, which resulted in 145 OTUs and 3252 DOMs, respectively. The network was then constructed with R packages "igraph" and "Hmisc" (Jr 2023; Csárdi et al. 2023). Only robust correlations with Spearman's correlation coefficients > 0.6 or < -0.6 and p value < 0.01 were retained. Besides, links among different DOMs were removed. The Gephi 0.9.2 (https://gephi.org/) was used to visualize the network and calculate topological properties such as average degree, average path length, density, betweenness, clustering coefficient, and modularity of the global network and degree and eigenvector centrality of each node. In particular, we employed the eigenvector centrality that assessed the significance of a node by taking into account the significance of its neighboring nodes (Golbeck 2013) to evaluate the importance of each DOM in the network. To assess the impact of deleting each DOM type on the property of the network produced above, 50% of each DOM component was randomly removed for 100 times (the function "sample" in R) and the subsequent networks was evaluated for the average path length using the R function "average.path.length" in package "igraph" (Csárdi et al. 2023).

3. Results

3.1. Phosphorus availability and iron reduction in the microcosm experiment

During the 25-day flooding incubation, soil Olsen-P content in all treatments increased over time (Figure 1a), indicating the activation and release of available P for plants. Specifically, the potential of Olsen-P supply (ΔOlsen-P) to plants increased by an average of 73% compared to unflooded conditions, with significantly higher levels observed in the NPK, CM(-P), and CM(P) treatments compared to CK, NK, and M(20%P) treatments (Figure S1). When assessing the activation efficiency (ratio of ΔOlsen-P to soil total P content), we found the highest activation efficiency of Olsen-P in the CM(P) treatment, followed by CM(-P), NPK, M(20%P), CK, and NK (Figure 1b).

The soil Fe(II) content in all treatments in the 25-day anaerobic incubation experiment was also increased similar to Olsen-P content and was significantly fitted to the logistic model (Figure 1c and Table S3). The CM(-P) and CM(P) treatments showed the highest iron reduction rates (Vmax) as 0.45 and 0.45 mg g-1 d-1, respectively, which were significantly higher than in the other treatments ($p < 0.05$, ANOVA with Tukey's HSD test) (Figure 1d and Table S3). Similarly, in the flooding condition, M(-P) and CM(P) treatments achieved Vmax in the shortest time (4.20 and 4.15 days, respectively), compared to other treatments (Table S3). It's worth noting that the maximum iron reduction potential (Pmax) was lower in the NPK treatment compared to that in other treatments, which exhibited a similar Pmax (Table S3).

 doi:10.20944/preprints202312.0664.v1

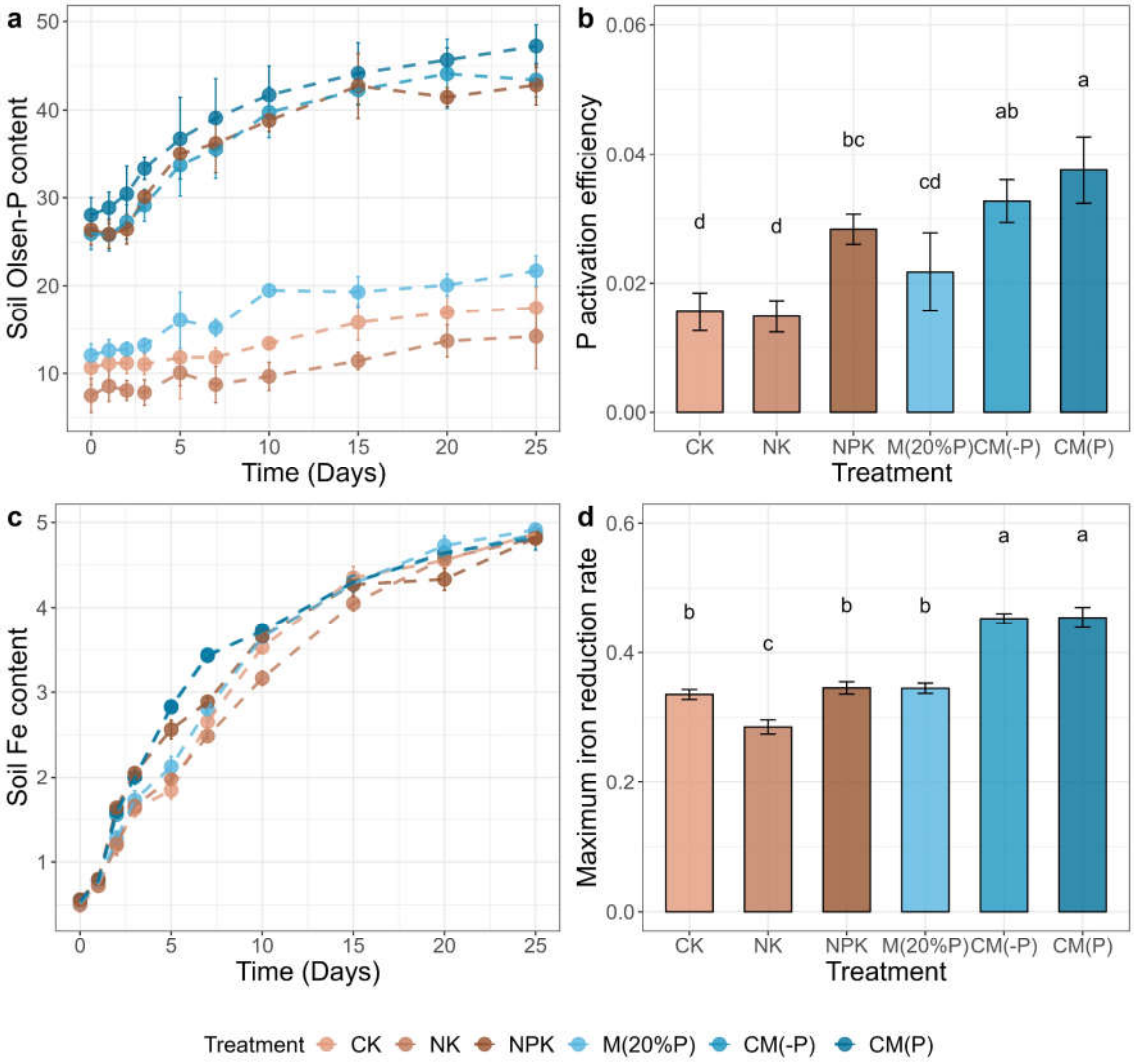

Figure 1. Soil Olsen-P and Fe(II) under anaerobic incubation. (a) The content of soil Olsen-P (mg kg-1) across 25 days. (b) The P activation efficiency under anaerobic flooding potential of Olsen-P supply to plant under anaerobic flooding, which calculated as the ratio of difference between the Olsen-P content of Days 0 and 25 to soil total P content (ΔOlsen-P/TP). (c) The content of soil Fe(II) (mg kg-1) across 25 days. (d) The maximum iron reduction rate (Vmax, mg g-1 d-1), assessed with logistics models for microbial Fe(III) reduction of soils. Error bar represents the standard deviation. Letters above bars indicate significant difference between treatments testing with ANOVA with Tukey's HSD test ($p < 0.05$).

We further assessed the role of P input, soil TP, and Fe(III) reduction on the Olsen-P activation efficiency with a variance partitioning analysis (VPA) analysis (Figure 2). This model was tested significantly ($p < 0.001$) with a residual of 19%. The finding showed that P input made a substantial and independent contribution of 16% towards to Olsen-P activation efficiency, which was higher than the other two components (i.e., 0% and 3% for TP and Vmax, respectively). Importantly, Olsen-P activation efficiency was explained jointly by Vmax and P input, accounting for 41% of the variance, and when considering all three components together, they collectively explained 19% of the variance. Overall, these results suggested that P input was the primary reason contributing to soil Olsen-P activation and supply, while Fe(III) reduction was largely responsible for P activation in paddy soil.

 doi:10.20944/preprints202312.0664.v1

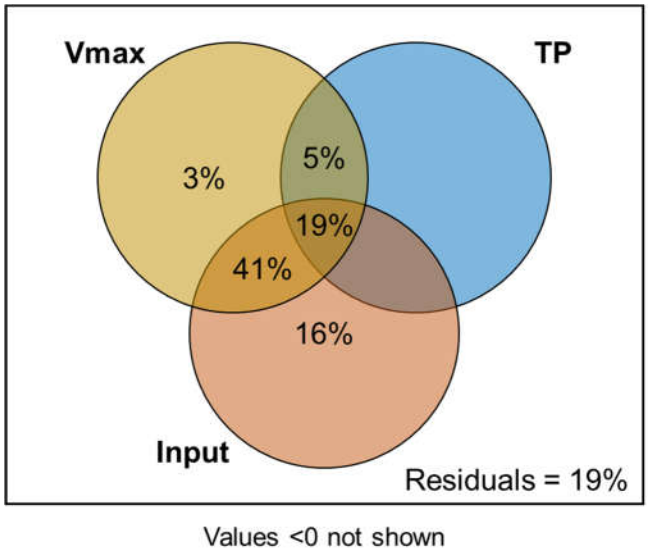

Figure 2. Variance Partitioning Analysis (VPA) revealed the essential role of Fe(III) reduction on Olsen-P activation efficiency in flooded soils. Vmax, the maximum iron reduction rate; TP, soil total P content; Input, total P input from fertilizers. The significance of the model was tested ($p < 0.001$, $n = 24$, degrees of freedom = 3).

3.2. Soil microbial communities under flooded conditions

The alpha-diversity and composition of soil microbial communities in anaerobic culture was assessed. The results showed that the soil contained a total of 37174 effective 16S rRNA gene sequences that assigned into 6542 OTUs. The average richness of all samples was 1998 and showed no significant difference among treatments ($p > 0.05$, ANOVA with Tukey's HSD test, Table S4). The Shannon diversity for the NPK treatment (7.28) was significantly lower compared to the other treatments ($p < 0.05$, ANOVA with Tukey's HSD test, Table S4).

Among all treatments, the dominant phyla were Firmicutes (29.03–47.58%), Planctomycetes (2.58–6.28%), Proteobacteria (1.62–4.53%), Chloroflexi (2.30–3.97%), and Actinobacteria (1.94–3.70%) (Figure 3a). At the genus level, Fonticella (2.26–6.81%), Clostridium_sensu_stricto_10 (1.86–5.56%), Aquisphaera (1.56–4.37%), Christensenellaceae_R_7_group (1.90–4.85%), and Ruminiclostridium (1.81–4.36%) were the dominant taxa of soil bacteria, and most of them were classified as Firmicutes. The PCoA analysis suggested that the composition of microbial community composition was significantly different among treatments ($p < 0.001$, Adonis test, Figure 3b). Within the 20 most abundant genera, we observed significant changes in relative abundance for six genera, which including Fonticella, Oxobacter, Bacillus, Desulfitobacterium, Anaerovorax, and Clostridium_sensu_stricto_1 (Figure 3c). Specifically, the abundance of these genera exhibited relatively higher abundances in both CK and NK treatments, whereas their relative abundance was lower in the NPK treatment. Compared to the NPK treatment, both the CM(-P) and CM(P) treatments significantly increased the relative abundance of Fonticella, Bacillus, Desulfitobacterium, and Clostridium_sensu_stricto_1 ($p < 0.05$, Figure 3c).

 doi:10.20944/preprints202312.0664.v1

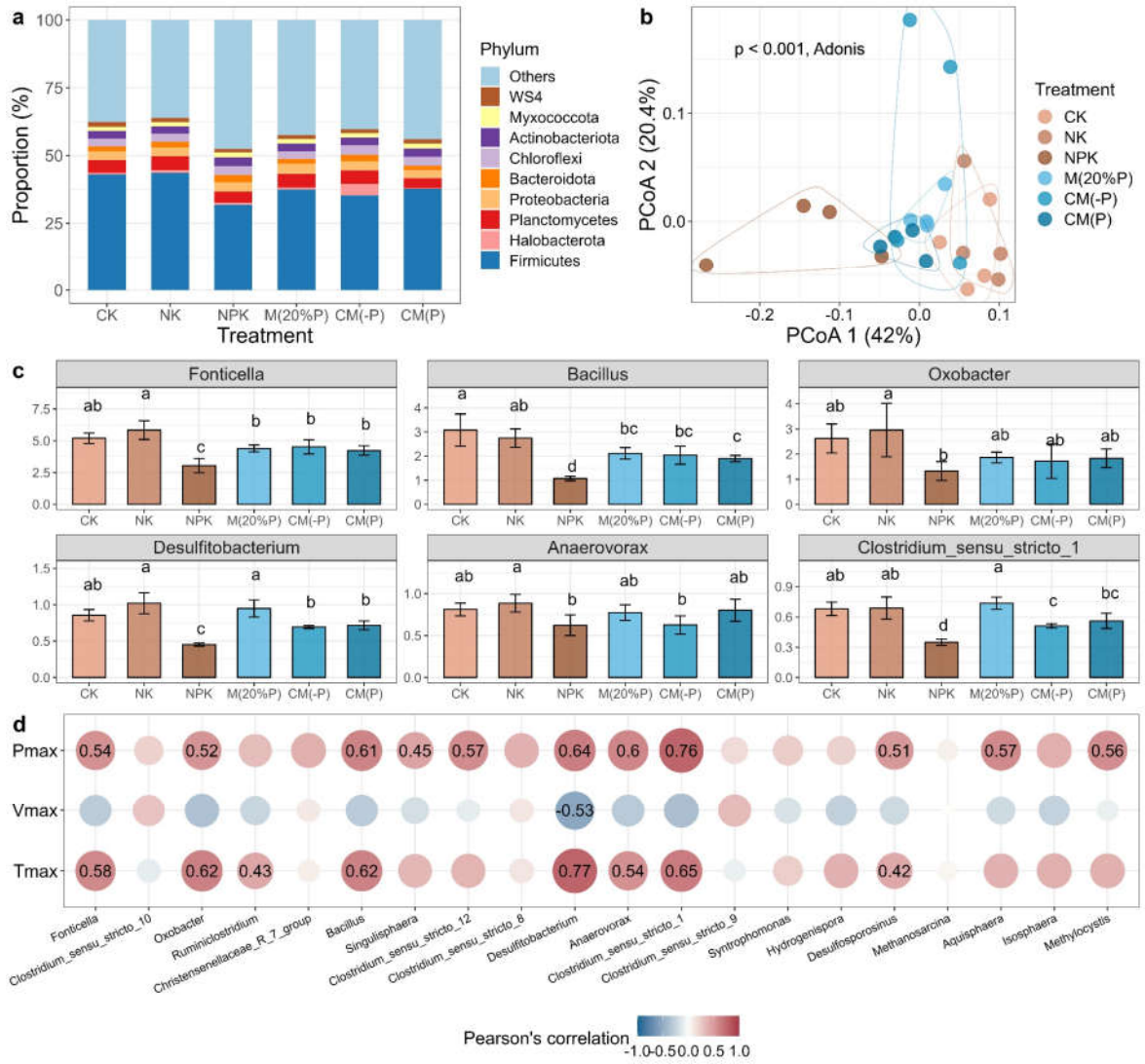

Figure 3. Soil microbial communities decoupled with soil Fe(III) reduction rate. (a) The relative abundance (%) of microbes at phylum level. (b) Principal Coordinates Analysis (PCoA) of bacterial composition. The difference of composition was assessed by a Permutational Multivariate Analysis of Variance (Adonis) test based on Bray-Curtis dissimilarity at 999 permutations. (c) Relative abundance (%) of dominant genera (out of 20 most abundant genera) with significantly different abundance among treatments. (d) The relative abundance of the iron-reducing bacteria failed to predict the Fe(III) reduction rate. Error bar represents the standard deviation. Letters above bars indicate significant difference between treatments testing with ANOVA with Tukey's HSD test ($p < 0.05$). The Pearson's correlation ($n = 24$) is used to assess the relationship between reduction parameters and bacterial abundance. Pmax, maximum iron reduction potential; Vmax, maximum iron reduction rate; Tmax, time to achieve the Vmax.

Given that soil bacteria are essential for Fe(III) reduction under anaerobic conditions, we conducted further investigations to assess the potential iron-reducing microbes by examining the relationship between three Fe(III) reduction parameters and the abundance of the 20 most abundant genera. The results showed that most of the genus positively correlated to the maximum iron reduction potential (Pmax), with eleven of those correlations were tested as significant ($p < 0.05$, Figure 3d). Similarly, the abundance of eight genera was significantly and positively correlated with the time taken to achieve the Vmax (Tmax). However, the correlations between the maximum iron reduction rate (Vmax) and genus abundance were non-significant, except for Desulfitobacterium.

 doi:10.20944/preprints202312.0664.v1

3.3. P limitation contributes to enrichment of iron-reducing bacteria

To delve deeper into the factors influencing the variation in iron-reducing bacterial abundance, we calculated the fold change in the relative abundance of each pair of samples and then correlated it with differences in Olsen-P and organic matter content. The results showed that the potential iron-reducing bacterial abundance (fold change) of all genera, except Clostridium_sensu_stricto_10, exhibited a significant and negative correlation with the Olsen-P (fold change) (Figure 4). This suggests that P limitation is the primary mechanism contributing to the increased abundance of potential iron-reducing bacteria in non-P-fertilized soils. Among these genera, Desulfitobacterium was found to have the strongest correlation coefficient (R = -0.71), followed by Clostridium_sensu_stricto_1 (R = -0.63), Bacillus (R = -0.57), and Clostridium_sensu_stricto_12 (R = -0.44), etc. In contrast, the relative abundance of potential iron-reducing bacteria (fold change) in four genera (Clostridium_sensu_stricto_9, R = 0.45; Desulfitobacterium, R = 0.29; Clostridium_sensu_stricto_1, R = 0.28; and Bacillus, R = 0.17) was significantly and positively correlated with the soil organic matter content (fold change) (Figure S2).

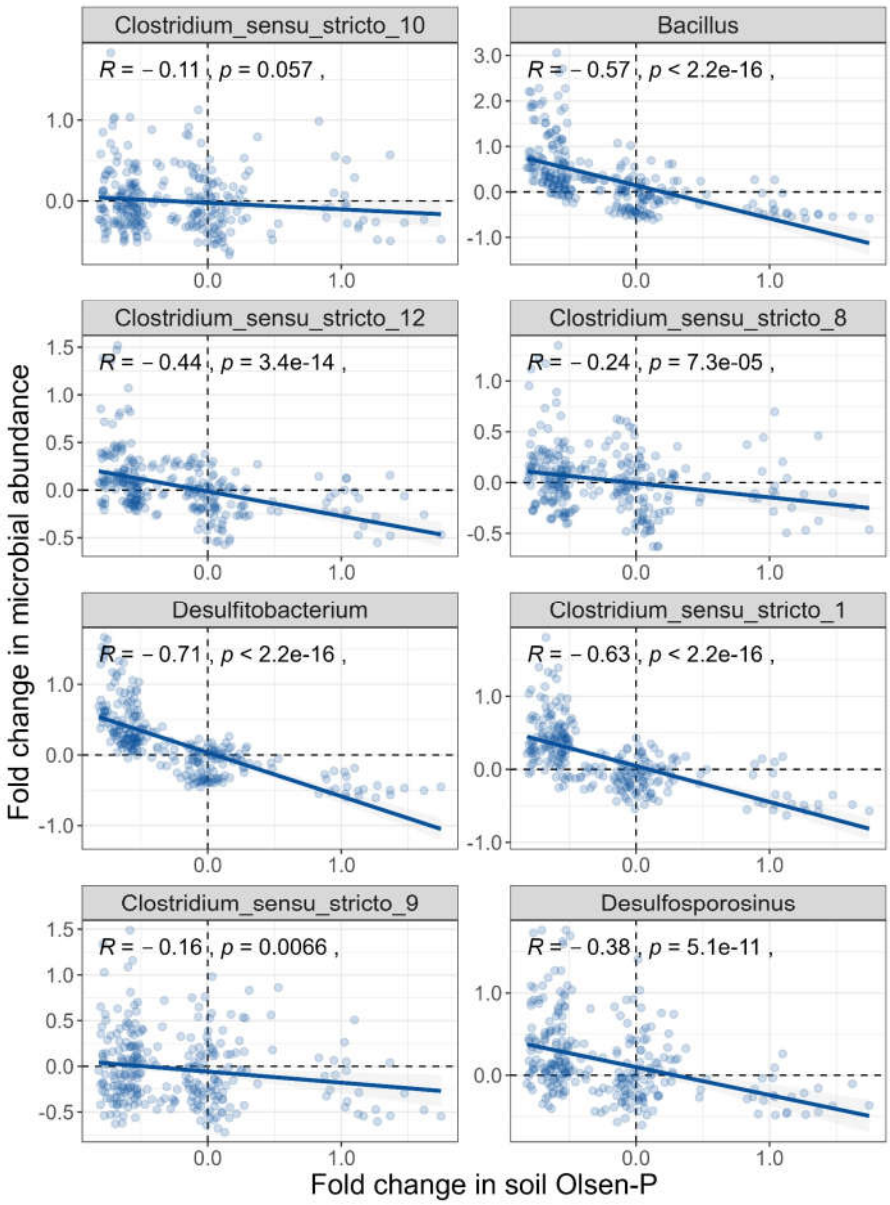

Figure 4. Soil P limitation contributes to enrichment of iron-reducing bacteria. The correlation between (pairwise) fold changes in soil Olsen-P and microbial relative abundance is assessed by Pearson's correlation.

 doi:10.20944/preprints202312.0664.v1

3.4. Soil DOM properties

FT-ICR-MS was used to further elucidate the molecular properties and composition of soil DOM in CK, NPK, and CM(-P) treatments. A total of 11868 organic molecules were detected across 12 samples, with an average of approximately 8300 molecules (Figure 5). Based on the O/C and H/C values depicted in in the van Krevelen diagram, DOM was categorized into 6 categories: lipids, unsaturated hydrocarbons, condensed polycyclic aromatics, proteins/amino sugars, lignin, tannins and carbohydrates (Figure 5a). Regarding the general properties of DOM, the CM(-P) treatment exhibited significant increases in the number of O atoms, mass-to-charge ratio (m/z), O/C ratio, and double bond equivalent value (DBE) in comparison to CK and NPK treatments ($p < 0.05$, ANOVA with Tukey's HSD test, Figure 5b). In contrast, the CM(-P) treatment significantly decreased the number of H atoms and H/C ratio compared to the CK treatment ($p < 0.05$, ANOVA with Tukey's HSD test, Figure 5b).

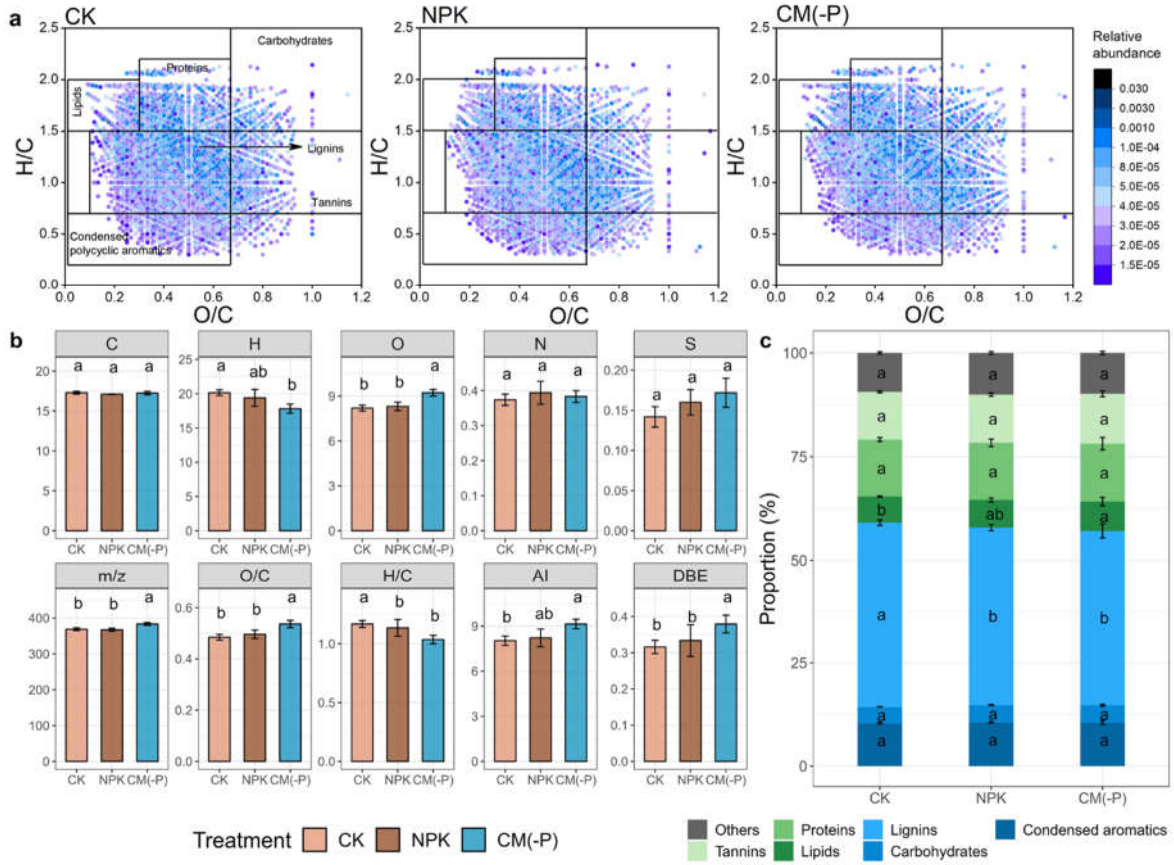

Figure 5. Soil DOM properties after four days of reflooding. (a) van Krevelen diagrams of DOM in soils. (b) Average formula atomic numbers for C, H, O, N, and S, mass-to-charge ratio (m/z), O/C and H/C atomic ratios, modified aromaticity index (AI), and double bond equivalent value (DBE) of all soil DOM. (c) The relative abundance of different DOM components. Error bar represents the standard deviation. Letters above bars indicate significant difference between treatments testing with ANOVA with Tukey's HSD test ($p < 0.05$, $n = 12$).

Regarding the composition of DOM compounds, soil DOM in all treatments was mainly composed of lignin, protein, condensed polycyclic aromatic and tannin compounds (~ 85%), with a minor presence of carbohydrates, lipids and others (Figure 5c). Under the CM(-P) treatment, the relative content of lignins was 49.30%, which was significantly lower than those in the CK (51.70%) treatment ($p < 0.05$, ANOVA with Tukey's HSD test, Figure 5c). The relative abundance of DOM compounds classified as others showed the opposite trend which was 9.09% under the CM(-P) treatment and was significantly higher than that in the CK treatment (8.26%, $p < 0.05$, ANOVA with Tukey's HSD test, Figure 5c).

 doi:10.20944/preprints202312.0664.v1

3.5. The relationship between soil DOM properties and iron reduction

Our results showed that the maximum iron reduction rate (Vmax) was significantly and positively correlated to the number of O and S atoms, O/C ratio, double bond equivalents (DBE), and modified aromaticity index (AI) of DOM (Table 1). Among DOM components, the relative abundance of lignins positively correlated with the Vmax (R = -0.57, p = 0.052). The significant and negative correlations between Vmax and DOM properties were observed for the number of H atom, H/C ratio. The correlations for Tmax were opposite to that of Vmax, especially for the relationship between Tmax and the relative abundance of lignins (R = 0.72, p = 0.008).

The correlation between P supply potential and efficiency to DOM properties showed similar as those for Vmax, but with relatively less significance (Table 1). Specifically, P supply efficiency was significantly and positively correlated to the number of O atom, O/C ratio, DBE, AI, and the relative abundance of DOM that classified as others. In contrast, the negative and significant correlations between P supply efficiency and DOM properties were observed for the number of H atom, H/C ratio, and the relative abundance of lignins.

3.6. Network analysis of associations between DOM and soil iron-reducing microbes

We performed the network analysis to investigate the associations between potential iron-reducing microbes (145 OTUs) and DOM (3253 molecules) (Figure S3). Within the network, there were a total of 4,899 links connecting 2,370 nodes, with 4,697 of these connecting DOM and iron-reducing microbes (Figure S3). There were 2,182 links indicating positive associations and 2,515 links indicating negative associations between DOM and microbes.

The centrality of each DOM in this network was calculated and used to reflect its importance to iron-reducing microbes. Notably, DOM with high centrality (> 0.1) tended to have relatively higher high molecular weights (> 300 Da) (Figure 6a). Zooming into the classification of DOM molecular, we found that DOM with high centrality (> 0.1) were mainly lignins (62%), followed by condensed aromatics (12%), and proteins/amino sugars (8%), (Figure S4). Interestingly, both the count and proportion of were decreased in other two groups with lower centrality (Figure S4). These results indicated that the crucial role of lingins in supporting iron-reducing microbes. A similar trend was also observed for carbohydrates and condensed aromatics. However, other DOM types, such as protein/amino sugars, tannins, and lipids showed the opposite trend (Figure S4).

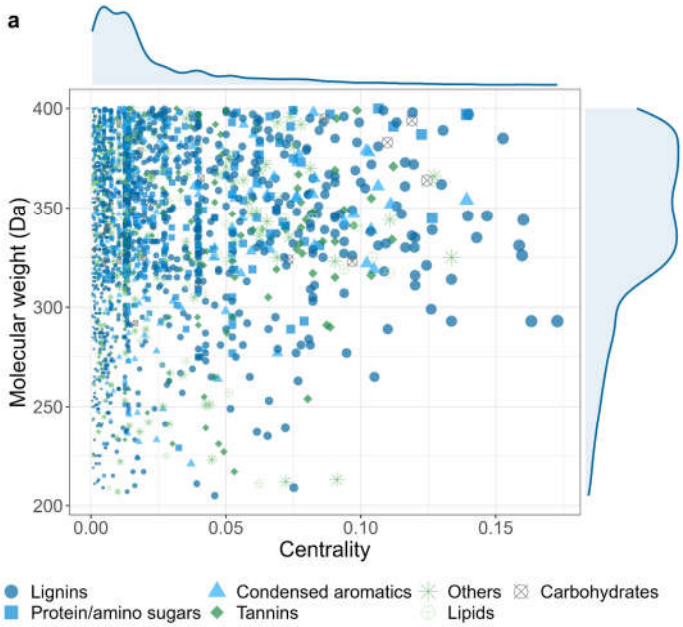

 doi:10.20944/preprints202312.0664.v1

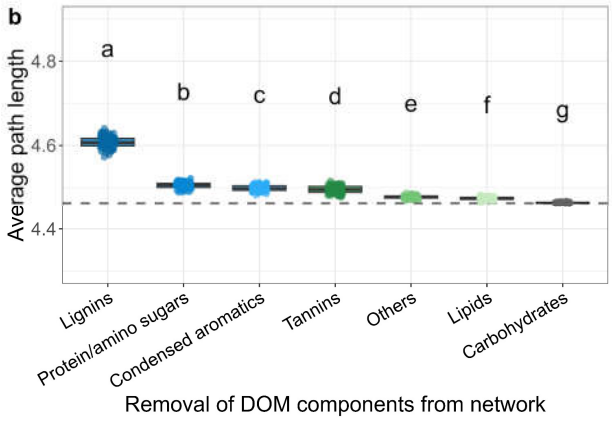

Figure 6. DOM's molecular weight and type determine its relationship to soil iron-reducing microbes. (a) The centrality of DOM within the correlation-based network of iron-reducing microbes and DOM. Centrality is a measure of the influence of a node in a network, reflecting the importance of DOM to iron-reducing microbes. The size of point indicates the value of centrality. (b) The average path length of networks after randomly deleting 50% of each DOM component from the original network. The random deletion was permutated 100 times generating 100 networks. Grey dash line indicates the average path length (4.46) of the original network. Letters indicate significant difference testing with ANOVA with Tukey's HSD test ($p < 0.05$).

The importance of each DOM type was further assessed by calculating the average path length of networks after randomly deleting 50% of corresponding DOM (Figure 6b). The results showed that deletion of certain DOM components will increase the average path length of the network, among which the path length of deletion of lignins was significantly higher than that of deletion of other components, indicating the importance of lignin in the association network of DOM and iron-reducing microbes (Figure 6b).

4. Discussion

4.1. The essential role of Fe(III) reduction on P activation in the flooded paddy soil

Phosphorus (P) in solutions often exhibits a high capacity for adsorption to iron (Fe) (hydr)oxides, leading to low P availability in soil (Borch and Fendorf 2007). The reduction of ferric iron (Fe(III)) may thus contribute to release of Fe(III)-bound P, whereas this was rarely reported. A recent study has shown that Fe(III)-bound P can serve as a relevant P source in rice production and microbe-driven P release from Fe (hydr)oxides can partially compensate for plant P requirements (Wang et al. 2022). In this study, by adding 32P-labeled ferrihydrite (30.8 mg P kg−1) into a paddy soil, it was reported that only 2% of 32P was recovered in rice plants, suggesting a small source of Fe(III)-bound P in rice production. However, our results show that the Olsen-P content increased by an average of 73% after 25-day flooding compared to unflooded soils, indicating the substantial activation of Fe(III)-bound P into the (potential) available P to plants. This large difference may be due to the fact that the Fe(III)-bound P already is largely present in the soil and can be taken up by plants following release, leading to lower detection of 32P. Moreover, soil microorganisms may have a greater propensity to reduce Fe(III) that is already present in the soil since this fraction may be largely coprecipitated with SOM and/or physically more accessible to them (Fritzsche et al. 2021).

The application of chemical phosphate fertilizers is intended to introduce large amounts of dissolved phosphorus into the soil. However, empirical observations suggested that the soil P use efficiency is often very low (15 - 30%) due to soil adsorption (Veneklaas et al. 2012). Indeed, this study reveals the significant but relatively weak effect of total P input on P activation, whereas the microbial iron reduction (reflected by the maximum iron reduction rate) collaboratively contributes to the P release in reflooded soils. This highlights the importance of microbial activities and the subsequent P release companied with iron reduction.

 doi:10.20944/preprints202312.0664.v1

4.2. The decoupling of Fe(III) reduction rate and iron-reducing microbes' abundance

Iron-reducing microbes represent a group of species that primarily responsible for controlling Fe(III) reduction process in various environments (Weber et al. 2006). The process of microbe-driven Fe(III) reduction is often coupled with the mineralization of soil organic matter (Merino et al. 2021; Kappler et al. 2021; Dong et al. 2023). These facts can easily lead to two reasonable conjectures: (1) the abundance of iron-reducing microbes would govern the Fe(III) reduction rate in the soil and (2) increasing soil organic matter would provide more resources for iron-reducing microbes and increase their abundance. Indeed, many studies speculated on Fe(III) reduction potential or rate by investigating the abundance of iron-reducing subgroups (Liu et al., 2019b; Chen et al., 2021; Liang et al., 2022). However, our results demonstrate that soil microbial composition significantly varied across treatments, with the CK and NK treatments significantly increased the abundance of iron-reducing microbes, such as Bacillus, Clostridium_sensu_stricto_1 and Desulfitobacterium. These genera are actually abundant in the current context that may largely regulate the Fe(III) reduction in reflooded soils (Weber et al. 2006; Ding et al. 2015). Additionally, other genera, such as Fonticella, Oxobacter, and Anaerovorax, also exhibited an increased abundance in the CK and NK treatments. Importantly, the abundance of main iron-reducing genera was not significantly correlated with the maximum Fe(III) reduction rate in soils, indicating the restrained functions of iron-reducing microbes in the CK and NK treatments.

By assessing the correlation between the relative abundance of potential Fe-reducing microbes' abundance and soil P and SOC contents, we further reveal that the depletion of P in soil significantly contributed to the increased abundance of Fe-reducing genera. This suggesting the crucial role of Fe-reducing microbes in P cycling, especially when the soil P pool is in a prolonged state of deficiency. This may explain the relative enrichment of iron-reducing microorganisms in the CK and NK treatments, where the soil had no exogenous P fertilizer input for up to 5 years. In contrast, the content of soil organic matter was identified as a positive but relatively weak factor influencing Fe-reducing microbes' abundance. This is consistent with the previously proposed conjecture and supports that the idea that interconnected processes of Fe–C cycling could be primarily regulated by Fe-reducing microbes (Dong et al. 2023).

4.3. Soil DOM accelerates microbe-driven Fe(III) reduction and P activation

SOM can affect the microbe-driven Fe(III) reduction by serving various roles such as electron donor, acceptor, shuttle, buffer or conductor (Dong et al. 2023). Our study demonstrates that soils treated with organic manure exhibit a higher maximum Fe-reduction rate and enhanced P activation efficiency. Additionally, we observed significant differences in the composition and properties of dissolved organic matter (DOM) among different treatments, and these differences are closely related to iron-reducing rate and P activation. These suggest that soil organic matter plays an integral role in microbe-driven Fe(III) reduction, particularly highlighting how the addition of organic manure accelerates the Fe(III) reduction rate and subsequently enhances P activation.

In this study, we had the innovative attempt on it by correlating the DOM composition with the traits of Fe(III) reduction and P activation. Our results show the decreased abundance of lignins under the organic manure treatment compared to the other two treatments, and this decrease exhibits significant and negative correlation with both the maximum Fe(III) reduction rate and P activation efficiency, whereas other components such as condensed aromatics and proteins/amino sugars showed opposite trends. However, this phenomenon is contrast to previous understanding of the effects of organic fertilizer additions on soil organic matter, i.e., that organic fertilizers, often containing lignin-rich exogenous additives, is expected to result in soil lignin enrichment (Bierke et al. 2008; Li et al. 2020; Yan et al. 2022). A plausible explanation for this may be linked to lignin decomposition occurring under the re-flooded condition of the soil following organic fertilizer application. Indeed, experiments in both the 30-year cultivated Mollisol and 11-year paddy soil demonstrated that pig manure applications promoted the microbial decomposition of plant lignin (Li et al. 2020; Zhou et al. 2022). Therefore, these studies suggest that lignin can be rapidly mineralized as a major carbon source for soil microorganisms following the addition of organic fertilizers.

Further exploration of the relationship between DOM molecules and iron-reducing microorganisms demonstrates that lignin is closely related to iron-reducing microorganisms. Lignin emerges as a key player in the network with iron-reducing microorganisms than other DOM components. Furthermore, our investigation highlights the significant centrality of high molecular weight organic matter in this network, underscoring its crucial role not only within the iron-reducing subgroup but also within the broader soil microbial community. This prominence may stem from the fact that the mineralization process of high molecular weight organic matter likely involves the cooperative action of numerous microorganisms, with the resulting metabolites serving as a resource for other microbes, thus exerting a more profound influence on the overall community. Likewise, the metabolites produced during the degradation of lignin may contribute to the accumulation of substances such as lipids and carbohydrates (Xu et al. 2019). Consequently, our research sheds light on the biochemical processes in reflooded paddy soil, where lignin decomposition, primarily driven by iron-reducing microbes, facilitates the P activation. However, it is important to note that future studies should aim to provide more direct evidence about the role of lignin degradation in Fe reduction. This could be achieved by introducing isotope-labeled lignin externally, enabling the tracking of microbial utilization of lignin and the identification of corresponding reaction substrates.

5. Conclusions

In summary, our study has provided a comprehensive understanding of the intricate interplay between carbon-iron-phosphorus (C-Fe-P) cycling dynamics within paddy soils and demonstrated that regulating microbial iron reduction through soil DOM content and properties can increase the available P release in paddy soils. This provides the pathway distinct from the physical processes elucidated in the context of soil P release and increased P availability (Wang et al., 2023) that is, high molecular weight DOM is shown to facilitate P release through the acceleration of the Fe reduction process. However, the C-Fe-P cycling may vary in different soils which relies on the abundance and activity of iron-reducing microbes and the P pools. Future research can continue to explore whether residual phosphorus utilization can be promoted through iron reduction processes and soil organic matter regulation, and investigate various fertilization and management measures for different soils.

Supplementary Materials: The following supporting information can be downloaded at the website of this paper posted on Preprints.org. The supplemental information includes the Figure S1-4 and Tables S1-5.

Funding: This work was supported by the National Natural Science Foundation of China (42077088) and the Zhejiang Province "Agriculture, Rural Areas, Rural People and Nine Institutions" Science and Technology Collaboration Program (2023SNJF039). X.P.L. was supported by a scholarship from the China Scholarship Council.

Data Availability: All the raw sequencing data have been deposited in the National Center for Biotechnology Information Sequence Read Archive under the accession number PRJNA756874.

Acknowledgments: Mr. Kunfeng Li (AES of Zhejiang University) is gratefully acknowledged for the assistance in soil sample collection.

Conflict of interest: The authors declare no conflicts of interest.

References

Abboud FY, Favaretto N, Motta ACV, et al (2018) Phosphorus mobility and degree of saturation in oxisol under no-tillage after long-term dairy liquid manure application. Soil Tillage Res 177:45–53. https://doi.org/10.1016/j.still.2017.11.014

Bi Q-F, Li K-J, Zheng B-X, et al (2020) Partial replacement of inorganic phosphorus (P) by organic manure reshapes phosphate mobilizing bacterial community and promotes P bioavailability in a paddy soil. Science of The Total Environment 703:134977. https://doi.org/10.1016/j.scitotenv.2019.134977

Bierke A, Kaiser K, Guggenberger G (2008) Crop residue management effects on organic matter in paddy soils — The lignin component. Geoderma 146:48–57. https://doi.org/10.1016/j.geoderma.2008.05.004

Borch T, Fendorf S (2007) Chapter 12 Phosphate Interactions with Iron (Hydr)oxides: Mineralization Pathways and Phosphorus Retention upon Bioreduction. In: Barnett MO, Kent DB (eds) Developments in Earth and Environmental Sciences. Elsevier, pp 321–348

Chen H, Ersan MS, Tolić N, et al (2022) Chemical characterization of dissolved organic matter as disinfection byproduct precursors by UV/fluorescence and ESI FT-ICR MS after smoldering combustion of leaf needles and woody trunks of pine (Pinus jeffreyi). Water Research 209:117962. https://doi.org/10.1016/j.watres.2021.117962

Chen S, Yang Y, Jing X, et al (2021) Enhanced aging of polystyrene microplastics in sediments under alternating anoxic-oxic conditions. Water Research 207:117782. https://doi.org/10.1016/j.watres.2021.117782

Cordell D, Drangert J-O, White S (2009) The story of phosphorus: Global food security and food for thought. Global Environmental Change 19:292–305. https://doi.org/10.1016/j.gloenvcha.2008.10.009

Csárdi G, Nepusz T, Traag V, et al (2023) igraph: Network Analysis and Visualization

Damon PM, Bowden B, Rose T, Rengel Z (2014) Crop residue contributions to phosphorus pools in agricultural soils: A review. Soil Biology and Biochemistry 74:127–137. https://doi.org/10.1016/j.soilbio.2014.03.003

Ding L-J, Su J-Q, Xu H-J, et al (2015) Long-term nitrogen fertilization of paddy soil shifts iron-reducing microbial community revealed by RNA-13C-acetate probing coupled with pyrosequencing. ISME J 9:721–734. https://doi.org/10.1038/ismej.2014.159

Dong H, Zeng Q, Sheng Y, et al (2023) Coupled iron cycling and organic matter transformation across redox interfaces. Nat Rev Earth Environ 4:659–673. https://doi.org/10.1038/s43017-023-00470-5

Fritzsche A, Bosch J, Sander M, et al (2021) Organic Matter from Redoximorphic Soils Accelerates and Sustains Microbial Fe(III) Reduction. Environ Sci Technol 55:10821–10831. https://doi.org/10.1021/acs.est.1c01183

Ge X, Wang L, Zhang W, Putnis CV (2020) Molecular Understanding of Humic Acid-Limited Phosphate Precipitation and Transformation. Environ Sci Technol 54:207–215. https://doi.org/10.1021/acs.est.9b05145

Golbeck J (2013) Chapter 3 - Network Structure and Measures. In: Golbeck J (ed) Analyzing the Social Web. Morgan Kaufmann, Boston, pp 25–44

Graves S, Dorai-Raj H-PP and LS with help from S (2019) multcompView: Visualizations of Paired Comparisons

He C, Zhang Y, Li Y, et al (2020) In-House Standard Method for Molecular Characterization of Dissolved Organic Matter by FT-ICR Mass Spectrometry. ACS Omega 5:11730–11736. https://doi.org/10.1021/acsomega.0c01055

He J, Qu D (2008) Dissimilatory Fe(III) reduction characteristics of paddy soil extract cultures treated with glucose or fatty acids. J Environ Sci (China) 20:1103–1108. https://doi.org/10.1016/s1001-0742(08)62156-7

Hiemstra T, Mia S, Duhaut P-B, Molleman B (2013) Natural and Pyrogenic Humic Acids at Goethite and Natural Oxide Surfaces Interacting with Phosphate. Environ Sci Technol 47:9182–9189. https://doi.org/10.1021/es400997n

Jindo K, Audette Y, Olivares FL, et al (2023) Biotic and abiotic effects of soil organic matter on the phytoavailable phosphorus in soils: a review. Chemical and Biological Technologies in Agriculture 10:29. https://doi.org/10.1186/s40538-023-00401-y

Jr FEH (2023) Hmisc: Harrell Miscellaneous

Kappler A, Bryce C, Mansor M, et al (2021) An evolving view on biogeochemical cycling of iron. Nat Rev Microbiol 19:360–374. https://doi.org/10.1038/s41579-020-00502-7

Koch BP, Dittmar T (2006) From mass to structure: an aromaticity index for high-resolution mass data of natural organic matter. Rapid Communications in Mass Spectrometry 20:926–932. https://doi.org/10.1002/rcm.2386

Koegel-Knabner I, Amelung W, Cao Z, et al (2010) Biogeochemistry of paddy soils. Geoderma 157:1–14. https://doi.org/10.1016/j.geoderma.2010.03.009

Kuczynski J, Stombaugh J, Walters WA, et al (2011) Using QIIME to analyze 16S rRNA gene sequences from Microbial Communities. Curr Protoc Bioinformatics CHAPTER:Unit10.7. https://doi.org/10.1002/0471250953.bi1007s36

Li J, Zhang X, Luo J, et al (2020) Differential accumulation of microbial necromass and plant lignin in synthetic versus organic fertilizer-amended soil. Soil Biology and Biochemistry 149:107967. https://doi.org/10.1016/j.soilbio.2020.107967

Li K, Bi Q, Liu X, et al (2022) Unveiling the role of dissolved organic matter on phosphorus sorption and availability in a 5-year manure amended paddy soil. Science of The Total Environment 838:155892. https://doi.org/10.1016/j.scitotenv.2022.155892

Li X-M, Sun G-X, Chen S-C, et al (2018) Molecular Chemodiversity of Dissolved Organic Matter in Paddy Soils. Environ Sci Technol 52:963–971. https://doi.org/10.1021/acs.est.7b00377

Liang Q, Chen T, Wang Y, et al (2022) Seasonal variation in release characteristics and mechanisms of sediment phosphorus to the overlying water in a free water surface wetland, southwest China. Environmental Pollution 308:119612. https://doi.org/10.1016/j.envpol.2022.119612

Liu X-P, Bi Q-F, Qiu L-L, et al (2019a) Increased risk of phosphorus and metal leaching from paddy soils after excessive manure application: Insights from a mesocosm study. Science of The Total Environment 666:778–785. https://doi.org/10.1016/j.scitotenv.2019.02.072

Liu Y, Dong Y, Ge T, et al (2019b) Impact of prolonged rice cultivation on coupling relationship among C, Fe, and Fe-reducing bacteria over a 1000-year paddy soil chronosequence. Biol Fertil Soils 55:589–602. https://doi.org/10.1007/s00374-019-01370-x

Liu Y, Zhu Z-Q, He X-S, et al (2018) Mechanisms of rice straw biochar effects on phosphorus sorption characteristics of acid upland red soils. Chemosphere 207:267–277. https://doi.org/10.1016/j.chemosphere.2018.05.086

Long Y, Hu X, Jiang J, et al (2021) Phosphorus sorption - Desorption behaviors in the sediments cultured with Hydrilla verticillata and Scripus triqueter as revealed by phosphorus fraction and dissolved organic matter. Chemosphere 271:129549. https://doi.org/10.1016/j.chemosphere.2021.129549

Menezes-Blackburn D, Paredes C, Zhang H, et al (2016) Organic Acids Regulation of Chemical–Microbial Phosphorus Transformations in Soils. Environ Sci Technol 50:11521–11531. https://doi.org/10.1021/acs.est.6b03017

Merino C, Kuzyakov Y, Godoy K, et al (2021) Iron-reducing bacteria decompose lignin by electron transfer from soil organic matter. Science of The Total Environment 761:143194. https://doi.org/10.1016/j.scitotenv.2020.143194

Oksanen J, Simpson GL, Blanchet FG, et al (2022) vegan: Community Ecology Package

Penn CJ, Camberato JJ (2019) A Critical Review on Soil Chemical Processes that Control How Soil pH Affects Phosphorus Availability to Plants. Agriculture 9:120. https://doi.org/10.3390/agriculture9060120

Qiu C, Feng Y, Wu M, et al (2019) NanoFe3O4 accelerates methanogenic straw degradation by improving energy metabolism. Bioresource Technology 292:121930. https://doi.org/10.1016/j.biortech.2019.121930

Quast C, Pruesse E, Yilmaz P, et al (2013) The SILVA ribosomal RNA gene database project: improved data processing and web-based tools. Nucleic Acids Res 41:D590–D596. https://doi.org/10.1093/nar/gks1219

Rivas-Ubach A, Liu Y, Bianchi TS, et al (2018) Moving beyond the van Krevelen Diagram: A New Stoichiometric Approach for Compound Classification in Organisms. Anal Chem 90:6152–6160. https://doi.org/10.1021/acs.analchem.8b00529

Sambrook J, Russell DW (2006) The condensed protocols from molecular cloning: a laboratory manual. Cold Spring Harbor Laboratory Press, Cold Spring Harbor, N.Y.

Schloss PD, Westcott SL, Ryabin T, et al (2009) Introducing mothur: open-source, platform-independent, community-supported software for describing and comparing microbial communities. Appl Environ Microbiol 75:7537–7541. https://doi.org/10.1128/AEM.01541-09

Takahashi Y, Katoh M (2022) Root response and phosphorus uptake with enhancement in available phosphorus level in soil in the presence of water-soluble organic matter deriving from organic material. Journal of Environmental Management 322:116038. https://doi.org/10.1016/j.jenvman.2022.116038

Tfaily MM, Hamdan R, Corbett JE, et al (2013) Investigating dissolved organic matter decomposition in northern peatlands using complimentary analytical techniques. Geochimica et Cosmochimica Acta 112:116–129. https://doi.org/10.1016/j.gca.2013.03.002

Veneklaas EJ, Lambers H, Bragg J, et al (2012) Opportunities for improving phosphorus-use efficiency in crop plants. New Phytologist 195:306–320. https://doi.org/10.1111/j.1469-8137.2012.04190.x

Wang C, Thielemann L, Dippold MA, et al (2022) Microbial iron reduction compensates for phosphorus limitation in paddy soils. Science of The Total Environment 837:155810. https://doi.org/10.1016/j.scitotenv.2022.155810

Wang H-B, Liu X-P, Jin B-J, et al (2023a) High-molecular-weight dissolved organic matter enhanced phosphorus availability in paddy soils: Evidence from field and microcosm experiments

Wang S-X, Huang Y-X, Wu Q-F, et al (2023b) A review of the application of iron oxides for phosphorus removal and recovery from wastewater. Critical Reviews in Environmental Science and Technology 0:1–19. https://doi.org/10.1080/10643389.2023.2242227

Weber KA, Achenbach LA, Coates JD (2006) Microorganisms pumping iron: anaerobic microbial iron oxidation and reduction. Nat Rev Microbiol 4:752–764. https://doi.org/10.1038/nrmicro1490

Wilfert P, Kumar PS, Korving L, et al (2015) The Relevance of Phosphorus and Iron Chemistry to the Recovery of Phosphorus from Wastewater: A Review. Environ Sci Technol 49:9400–9414. https://doi.org/10.1021/acs.est.5b00150

Xu Z, Lei P, Zhai R, et al (2019) Recent advances in lignin valorization with bacterial cultures: microorganisms, metabolic pathways, and bio-products. Biotechnology for Biofuels 12:32. https://doi.org/10.1186/s13068-019-1376-0

Yan M, Zhang X, Liu K, et al (2022) Particle size primarily shifts chemical composition of organic matter under long-term fertilization in paddy soil. European Journal of Soil Science 73:e13170. https://doi.org/10.1111/ejss.13170

Yan Z, Chen S, Li J, et al (2016) Manure and nitrogen application enhances soil phosphorus mobility in calcareous soil in greenhouses. Journal of environmental management 181:26–35. https://doi.org/10.1016/j.jenvman.2016.05.081

Yang Y, Zhang H, Qian X, et al (2017) Excessive application of pig manure increases the risk of P loss in calcic cinnamon soil in China. The Science of the total environment 609:102–108. https://doi.org/10.1016/j.scitotenv.2017.07.149

 doi:10.20944/preprints202312.0664.v1

Yao Y, Wang L, Hemamali Peduruhewa J, et al (2023) The coupling between iron and carbon and iron reducing bacteria control carbon sequestration in paddy soils. CATENA 223:106937. https://doi.org/10.1016/j.catena.2023.106937

Yin Y, Liang CH (2013) Transformation of phosphorus fractions in paddy soil amended with pig manure. Journal of Soil Science and Plant Nutrition 13:809–818

Zhang S, Wang L, Chen S, et al (2022) Enhanced phosphorus mobility in a calcareous soil with organic amendments additions: Insights from a long term study with equal phosphorus input. Journal of Environmental Management 306:114451. https://doi.org/10.1016/j.jenvman.2022.114451

Zheng B-X, Ding K, Yang X-R, et al (2019) Straw biochar increases the abundance of inorganic phosphate solubilizing bacterial community for better rape (Brassica napus) growth and phosphate uptake. Science of The Total Environment 647:1113–1120. https://doi.org/10.1016/j.scitotenv.2018.07.454

Zhou J, Wu L, Deng Y, et al (2011) Reproducibility and quantitation of amplicon sequencing-based detection. ISME J 5:1303–1313. https://doi.org/10.1038/ismej.2011.11

Zhou Y, Zhang J, Xu L, et al (2022) Long-term fertilizer postponing promotes soil organic carbon sequestration in paddy soils by accelerating lignin degradation and increasing microbial necromass. Soil Biology and Biochemistry 175:108839. https://doi.org/10.1016/j.soilbio.2022.108839

Zhu J, Li M, Whelan M (2018) Phosphorus activators contribute to legacy phosphorus availability in agricultural soils: A review. Science of the Total Environment 612:522–537. https://doi.org/10.1016/j.scitotenv.2017.08.095